Preparation of BaTiO$_3$-Based Nonreducible X7R Dielectric Materials Via Nanometer Powders Doping

Xiaohua Zhou · Shuren Zhang · Ying Yuan · Bo Li · Jingsong Liu

Abstract Nonreducible X7R dielectric materials, which can be cofired with Ni electrode, were obtained by doping nanometer additives to BaTiO$_3$ powders synthesized by employing a sol-gel method. The crystallization process, structure and constituent of nanometer additives, as well as morphologies were studied via differential thermal and thermogravimetric analyses (DTA/TG), X-ray diffraction (XRD) and transmission electron microscopy (TEM). The effects of the calcining temperature of dopants on the dielectric properties were also discussed. The experiment results proved that higher-performance X7R dielectric materials could be obtained via nanometer doping compared with conventional doping. At room temperature, dielectric constant is more than 3000; dielectric loss lower than 1.0% and insulation resistance more than $10^{11}\,\Omega\cdot$cm.

1. Introduction

Recently, the driving forces on multilayer ceramic capacitors (MLCC) technologies are increasing due to the rapid growth of market demands and requirements for miniaturization, high volumetric efficiency, high performance, high reliability and low cost [1]. The effective approaches to achieve high-performance MLCC with small size include using higher permittivity dielectrics, reducing dielectric layer thickness and increasing the number of stacked layers. However, with the decrease of dielectric layer thickness, it is essential to reduce the particle size of raw materials. For the conventional solid-state method, additives with small amounts are usually me-

X. Zhou · S. Zhang · Y. Yuan (✉) · B. Li · J. Liu
School of Microelectronic and Solid State Electronic, University of Electronic Science and Technology of China, Chengdu, 610054, People's Republic of China
e-mail: yingyuan@uestc.edu.cn

chanically blended with the major phase, but it is difficult to achieve uniform distribution of the additives by this method, particularly if the particle size of additives is comparable with that of the main component. Many techniques have been developed to achieve a homogenous distribution of dopants in BaTiO$_3$ (BT) powders, such as sol-gel coating of powders [2], solution coating of powders [3] and direct sol-gel synthesis of doped powders [4]. However, these methods are restricted in the industry manufacture of MLCC materials, due to the disadvantages, such as complex process, long production cycle and expensive raw materials.

Conventionally, Ni-MLCC X7R materials are prepared through mixing BT powders with compounds of Mg, Y, Co and Mn. In addition, (Ba$_x$ Ca$_y$)SiO$_3$ is used as sintering aid to lower sintering temperature. This study is devoted to fabricate Ni-MLCC materials through doping nanometer additives synthesized by a sol-gel method. Experiment results proved that it was favorable to use this kind of dopants to form homogenous "core-shell" microstructure and achieve high-performance Ni-MLCC dielectric materials.
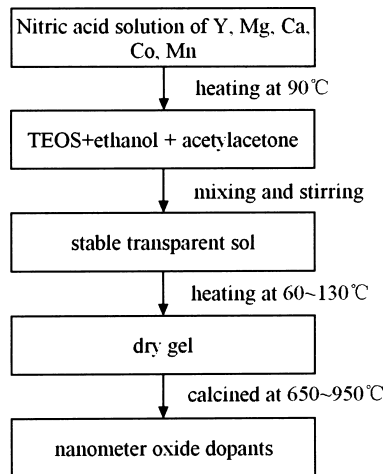
2. Experimental Procedure

2.1. Sample preparation

Commercial BT powders were synthesized by a hydrothermal method with an average particle size of ~0.4 μm and a specific surface area of 2.68 m^2/g. Yttrium oxide (purity: >99.95%), cobalt nitrate (>99%), manganese nitrate (>99%) and carbonates of calcium and magnesium (>99.5% purity) were used as starting materials and dissolved in nitric acid solution. Tetraethyl silicate (TEOS, >98.0%) was used to introduce silicate element. Ethanol and acetylacetone were chosen to be solvent and stabilizer, respectively. Fig. 1

Table 1 Influence of temperatures on the sol formation

Temperature (°C)	Sol formation
$T \leq 80°C$	Solution demixing
$80°C \leq T \leq 90°C$	Homogeneous and transparent sol
$90°C \leq T$	Mass smoke and SiO_2 particle appeared

Fig. 1 Flow chart for the synthesis of nanometer dopants

Fig. 2 DTA/TG curves of dry gel

3. Results and Discussion

Fig. 2 shows the results of DTA/TG analyses of the dry gel. For DTA curve, there are two endothermic peaks and three exothermic peaks. The first endothermic peak (peak A, strong) appears at about 120°C, attributed to the evaporation of surface absorbed water, dehydration of crystal water and volatilization of organic solvent. The second endothermic peak at 350°C (peak C, weak) was due to the decomposition of nitrates and formation of polymer via hydrolyzing-polymerization. In addition, the exothermic peaks appear at 280°C, 510°C and 850°C, respectively, among which, the first one (peak B) was caused by burning of organic substances; the second (peak D) was corresponding to the formation of amorphous silicates via solid state reaction, and the last one (peak E) was regarded as the crystallization of silicates. For TG curve, it shows a majority weight loss below 500°C and there is no loss in weight thereafter. Thus, it could be concluded that combustion and decomposition of the dry gel and the crystallization of silicates have been finished at 850°C.

Fig. 3 shows the XRD curves of the dopants calcined at 650°C, 750°C, 850°C and 950°C, respectively. Broad peaks

shows the flow chart for the fabrication process of nanometer dopants. Nitric acid and TEOS ethanol solutions were mixed with an appropriate proportion and at an appropriate temperature. Table 1 shows the influence of temperature on the sol formation. Further stirring was performed to make the mixed solutions homogenous and form uniform sol. Sol could transform to transparent gel via heating at 60°C and dry gel was obtained via further heating at 130°C. Finally, dry gel precursors were calcined at different temperatures to obtain nanometer dopants.
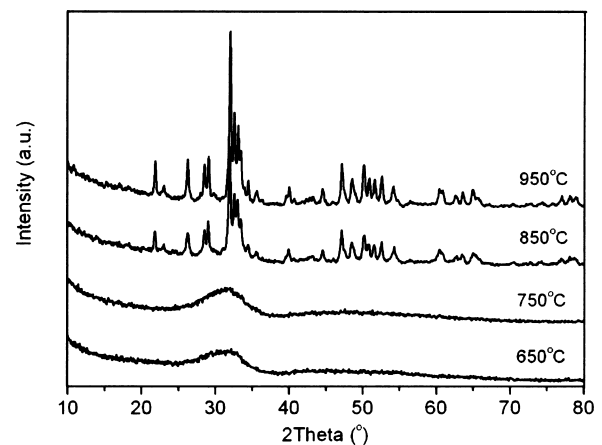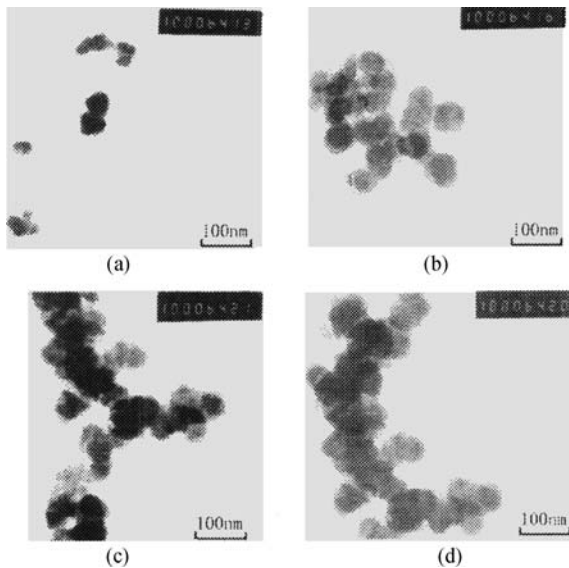
2.2. Measurement

Differential thermal and thermogravimetric analyses (DTA/TG, Model DSC2910) were used to investigate the process of crystallization within a temperature range of 30°C ~1, 200°C, at a heating rate of 5°C/min and an air flow rate of 50 ml/min.. The phase identification and structure analysis for the nanometer powders that were synthesized at different temperatures were performed via powder X-ray diffraction (XRD, Model D/MAX-IIIA). Particle size was determined by transmission electron microscopy (TEM, Model JSM-35C). Temperature characteristics of dielectric constant were measured with an impedance analyzer (Model HP4192A). The temperature range of measurement varied from −25°C to 130°C, with a heating rate of 2°C/min.

Fig. 3 XRD patterns of dopants calcined at different temperatures (a) 650°C (b) 750°C (c) 850°C (d) 950°C for 2 h

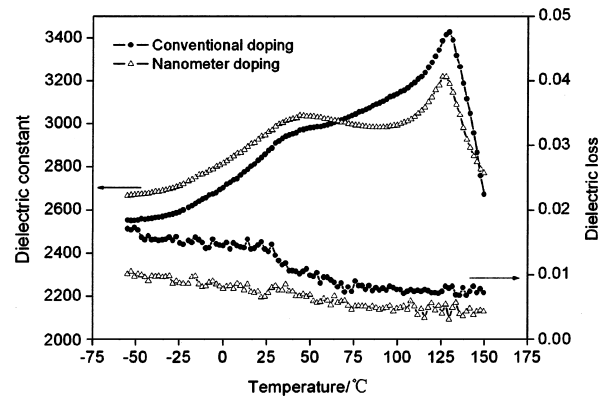**Fig. 4** TEM of dopants calcined at different temperatures (a) 650 °C (b) 750 °C (c) 850 °C (d) 950 °C

Fig. 5 Temperature dependences of dielectric constant and dielectric loss of materials prepared by conventional doping and nanometer doping

were observed at about 33° for the samples calcined below 750°C, which indicated the formation of amorphous silicates. Crystalline silicates formation occurred above 750°C and the compound calcined at 850°C was identified to $Y_4MgSi_3O_{13}$ with a hexagonal symmetry (JCPDS 20-1410), which was in consistency with the exothermic peak at 850°C on DTA curve. Further increases of the calcining temperature made the diffraction peaks sharp, as a result of both the increase of the fraction of crystalline silicates and their grain growth.

The particle sizes and morphologies of the dopants calcined at different temperatures were observed with TEM, as shown in Fig. 4. All dopants particles exhibited basically spherical morphologies, with an average size of 25–70 nm. From the analyses of Figs. 3 and 4, the average particle size increased with the calcining temperature, simultaneously, the amorphous-crystalline transition for nanometer dopants took place.

Fig. 5 compares the temperature dependences of dielectric constant and dielectric loss for ceramic samples prepared by conventional and nanometer doping methods, respectively.

Compared with conventional doping, the room temperature permittivity increased and the dielectric constant at Curie temperature (T_c) decreased via nanometer doping, and the T_c shifted from 130°C to 126°C. It was also observed that the dielectric loss was depressed to a great extent via doping nanometer powders. It is well known that temperature-stable dielectrics based on BT have a "core-shell" structure, which consists of a tetragonal ferroelectric unreacted core and a paraelectric modified shell [5–8]. The dielectric peak at T_c is associated with the ferroelectric-paraelectric transition of unreacted pure $BaTiO_3$ grain core, and the volume fraction of grain shell is responsible for the dielectric constant at room temperature [9]. For conventional doping, sub-

micron size dopants were utilized, which could not disperse homogeneously in BT powders with a comparative particle size so that the quantity of grains with a "core-shell" structure was limited. However, abundant grains formed a "core-shell" structure, due to the uniform distribution of nanometer dopants in BT with a relatively small size [10]. Furthermore, the volume fraction of grain core decreased while that of grain shell increased by nanometer doping as compared with conventional doping, due to a large specific area, high interfacial energy and strong tendency to incorporate into $BaTiO_3$ lattice of nanometer dopants. Thus, flatter temperature characteristic (TC) of the permittivity and relatively high dielectric performance were obtained via nanometer doping. Nonreducible BT-based ceramic materials with excellent dielectric properties, i.e. $\varepsilon_{298K} > 3000$, $tg\delta \le 1.0\%$, $\rho \ge 10^{12}\Omega\cdot cm$ were achieved by means of nanometer doping and satisfied the requirements of EIA X7R specification.

Fig. 6 shows the TC of ceramics doped with the same amount of nanometer powders calcined at 650°C and 950°C, respectively. It was obvious that the ceramic doped with powders calcined at 650°C showed lower dielectric constant,
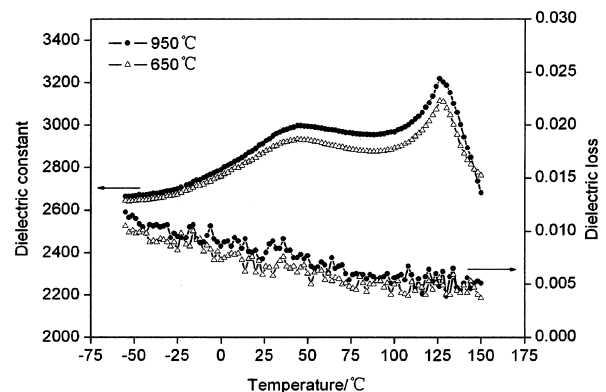
Fig. 6 Temperature dependences of dielectric constant and dielectric loss of materials doped with nanometer powders calcined at different temperatures

dielectric loss and variation rate of capacitance. From the analyses of XRD and TEM, the nanometer dopants transformed from amorphous to crystalline state and the average particle size increased with the calcining temperature. Thus, the dopants were amorphous when they were calcined at 650°C, whereas they transformed to crystal when they were calcined at 950°C. Therefore, the dopants calcined at 650°C exhibited more activities to diffuse into BaTiO₃ lattice and were helpful to form a "core-shell" structure, resulting in decrease of the dielectric constant and flatter temperature characteristic. Moreover, the noncrystalline dopants could promote the densification process of ceramic, as a result of the formation of liquid phase as sintering aid in sintering process. Consequently, the dielectric loss was depressed by doping powders that were calcined at 650°C.

4. Conclusions

This paper investigated a novel technique to fabricate nonreducible BaTiO₃-based ceramic materials. The silicates of Y, Mg, Ca, Co and Mn were prepared by a sol-gel method via heat treatment at 650–950°C and used as dopants. DTA/TG and XRD analyses proved that the silicates calcined at 650°C were amorphous and the crystalline silicates began to form above 750°C. The dopants calcined at 650°C to 950°C were composed of very fine particles, and the average particle size increased from about 25 to 70 nm as the calcining temperature increased. The dopants synthesized at 650°C were proven favorable to form a "core-shell" structure and promote the densification process of ceramics, resulting in a flatter TC of the permittivity and depressed dielectric loss. High-performance X7R dielectric materials could be developed by this method, with an enhanced room-temperature dielectric constant, a depressed dielectric loss and a high insulation resistance, i.e. $\varepsilon_{298k} > 3000$, $tg\delta \leq 1.0\%$, $\rho \geq 10^{12}\Omega\cdot$cm, as compared with the conventional doping method. This method is hopeful to the production of X7R Ni-MLCC materials.

References

1. H. Kishi, Y. Mizuno, H. Chazono, Jpn. J. Appl. Phys. **42**, 1 (2003)
2. F.A. Selmi, V.R. Amarakoon, J. Am. Ceram. Soc. **71**, 934 (1988)
3. S.A. Bruno, D.K. Swanson, J. Am. Ceram. Soc. **76**, 1233 (1993)
4. D. Hennings, P. Hansen, "Ceramic multilayer capacitor". US Pat. No. 6072688, 2000.
5. D. Hennings, G. Rosenstein, J. Am. Ceram. Soc. **67**, 249 (1984)
6. H. Chazono, M. Fujimoto, Jpn. J. Appl. Phys. **34**, 5354 (1995)
7. H. Kishi, Y. Okino. M. Honda, et al., Jpn. J. Appl. Phys. **36**, 5954 (1997)
8. H. Kishi, N. Kohzu, J. Sugino, et al., J. Eur. Ceram. Soc. **19**, 1043 (1999)
9. Y. Park, Y.H. Kim, H.G. Kim, Mat. Lett. **28**, 101 (1996)
10. Y. Yuan, S.R. Zhang, W.N. You, Mat. Lett. **58**, 1959 (2004)